Published in final edited form as:
Neuron. 2008 October 23; 60(2): 308–320. doi:10.1016/j.neuron.2008.08.012.

Synaptic signaling by all-trans retinoic acid in homeostatic synaptic plasticity

Jason Aoto[1,*], **Christine I. Nam**[1,*], **Michael M. Poon**[1,*], **Pamela Ting**[1], and **Lu Chen**[1,2,†]

[1]Department of Molecular and Cell Biology, University of California, Berkeley, California 94720-3200

[2]Helen Wills Neuroscience Institute, University of California, Berkeley, California 94720-3200

SUMMARY

Normal brain function requires that the overall synaptic activity in neural circuits be kept constant. Long-term alterations of neural activity leads to homeostatic regulation of synaptic strength by a process known as synaptic scaling. The molecular mechanisms underlying synaptic scaling are largely unknown. Here we report that all-trans retinoic acid (RA), a well-known developmental morphogen, unexpectedly mediates synaptic scaling in response to activity blockade. We show that activity blockade increases RA synthesis in neurons, and that acute RA treatment enhances synaptic transmission. The RA-induced increase in synaptic strength is occluded by activity blockade-induced synaptic scaling. Suppression of RA synthesis prevents synaptic scaling. This novel form of RA signaling operates via a translation-dependent but transcription-independent mechanism, causes an up-regulation of postsynaptic glutamate receptor levels, and requires RARα receptors. Together, our data suggest that RA functions in homeostatic plasticity as a signaling molecule that increases synaptic strength by a protein synthesis-dependent mechanism.

INTRODUCTION

Normal nervous system function requires that neurons maintain a constant overall activity level and maintain a balance between the relative strength of individual synapses. Constant neural activity levels are achieved by synaptic scaling, a form of homeostatic synaptic plasticity (Davis, 2006; Turrigiano and Nelson, 2004). In synaptic scaling, all synapses of a neuron are modified concurrently in a multiplicative fashion with greater synaptic adjustment to stronger synapses, thereby preserving the relative synaptic weights of the overall circuit (Thiagarajan et al., 2005; Turrigiano et al., 1998) (but see Echegoyen et al., 2007). Several signaling pathways have been shown to mediate various forms of homeostatic synaptic plasticity in the mammalian central nervous system and the *Drosophila* neuromuscular junction. A decrease in neuronal activity, for instance, has been shown to decrease the ratio of α/ β Ca–MKII protein in neurons, likely by upregulating transcription of βCaMKII (Thiagarajan et al., 2002). The level of Arc/Arg3.1, an immediate-early gene that is rapidly induced by neuronal activity associated with information encoding in the

[†]Address correspondence to: Lu Chen, Department of Molecular and Cell Biology, University of California, 201 LSA, MC 3200, Berkeley, CA 94720-3200, Phone: (510)643-8163, Fax: (510)643-6791, e-mail: luchen@berkeley.edu.
[*]These authors contributed equally to this work.

brain (Guzowski et al., 2005), modulates homeostatic plasticity through a direct interaction with the endocytic pathway (Shepherd et al., 2006). At the *Drosophila* neuromuscular junction, homeostatic synaptic growth is regulated by TGF-β, a synaptically released growth factor (Sweeney and Davis, 2002). In addition to these neuron/muscle-autonomous factors, glia-derived factors such as the cytokine TNFα was demonstrated to control synaptic strength, and to influence homeostatic synaptic plasticity (Beattie et al., 2002; Stellwagen and Malenka, 2006).

One particularly well-characterized form of homeostatic plasticity is the increase in synaptic strength induced by chronic blockade of neuronal activity with tetrodotoxin (TTX) and the NMDA receptor antagonist APV. A series of recent studies indicate that this form of homeostatic plasticity is mediated by the local synthesis and synaptic insertion of homomeric GluR1 receptors, which results in an increase of synaptic glutamate receptor response as manifested in an enhanced amplitude of unitary spontaneous miniature EPSCs (Ju et al., 2004; Sutton et al., 2006; Sutton et al., 2004). Although several biochemical signaling pathways that trigger dendritic protein synthesis upon increase in neuronal activity have been identified (Kelleher et al., 2004; Klann and Dever, 2004; Schuman et al., 2006), signaling pathways involved in this type of inactivity-induced synaptic scaling remain to be determined.

During development, all-trans retinoic acid (RA) regulates gene transcription by binding to retinoic acid receptor (RAR) proteins, which are well-characterized transcription factors of the nuclear receptor family. In the nervous system, RA signaling is involved in neurogenesis and neuronal differentiation. Increasing evidence indicates that RA signaling may also play an important role in the mature brain (Lane and Bailey, 2005). Specifically, RA is rapidly synthesized in various regions of the adult brain (Dev et al., 1993). Deficiencies in retinoid metabolism and signaling cause impaired synaptic plasticity and learning (Chiang et al., 1998; Cocco et al., 2002; Misner et al., 2001), and may result in neurological diseases (Lane and Bailey, 2005). Consistent with the notion that RA may have a role in the postmitotic properties of neurons, a recent study suggested that RA induces spine formation in cultured neurons by binding to a novel, cell surface-exposed variant of the RA-receptor RARα (Chen and Napoli, 2008).

Here we report that RA is a potent regulator of synaptic strength in cultured neurons and brain slices. We demonstrate that activity blockade – which induces homeostatic plasticity – strongly stimulates neuronal RA synthesis. We also show that RA rapidly increases synaptic strength, and that activity-dependent synaptic up-scaling occludes the subsequent RA-induced increase in synaptic strength. In addition, knocking down RARα expression in neurons using shRNA blocked both RA-induced and activity blockade-nduced synaptic scaling. Direct activation of RARα with a selective agonist mimics the effect of RA, indicating the essential involvement of RARα in homeostatic plasticity. In our experiments, the synaptic effect of RA is independent of the formation of new dendritic spines, but instead operates by stimulating the synthesis and insertion of new postsynaptic glutamate receptors in existing synapses. Our results thus suggest that RA functions as a novel synaptic signal that operates via RARα during homeostatic plasticity to upregulate synaptic strength by increasing the size of the postsynaptic glutamate receptor response.

RESULTS

RA mediates scaling of excitatory synaptic transmission

We examined synaptic transmission in hippocampal pyramidal neurons from 5–7 day-in-vitro (DIV) cultured slices. Two hours after the addition of RA (1 μM) to the culture media, a significant increase in miniature excitatory postsynaptic current (mEPSC) amplitude was

observed in comparison to DMSO-treated neurons (Figures 1A and B). The mEPSC frequency was not changed by RA treatment. The rapid time course of the RA effect on synaptic transmission was somewhat surprising, raising the question whether we could observe a similar phenomenon in dissociated cultured neurons. Indeed, a significant increase in mEPSC amplitude was induced in primary cultured hippocampal neurons as early as an hour after a 30 min treatment with RA (Figure 1C). Similar to the results from cultured slices, this RA-induced increase in synaptic transmission did not involve an increase in mEPSC frequency (Figures 1F), suggesting a postsynaptic mechanism. Analysis of the mEPSC amplitude distributions after DMSO or RA treatments showed that the RA-induced increase in synaptic strength was multiplicative, rather than additive (Figure 1D and E; compare green dots with dashed line in 1D), reminiscent of synaptic scaling induced by reduced network activity (Thiagarajan et al., 2005; Turrigiano et al., 1998). A recent report suggested that RA induces rapid spine formation by a mechanism that involves activation of the RA-receptor RARα exposed on the cell surface (Chen and Napoli, 2008). However, we observed no increase in spine density upon RA treatment (Figures 1G and S1), consistent with the lack of change in mEPSC frequency. Thus, at least under our conditions, RA causes a functional change in existing synapses without a major induction of new spines and synapses.

Intrigued by the synaptic upscaling induced by RA, we next directly asked whether RA is involved in activity blockade-induced homeostatic synaptic plasticity. To test this question, we applied citral, an inhibitor of retinol dehydrogenase (ROLDH) (Di Renzo et al., 2007; Song et al., 2004; Tanaka et al., 1996), the enzyme that oxidizes all-trans-retinol to all-trans-retinal in the synthetic pathway of RA (Lane and Bailey, 2005). Consistent with previous studies (Ju et al., 2004; Sutton et al., 2006; Sutton et al., 2004), we found that blocking neuronal activity with TTX and APV for 24 hours induced a significant increase in mEPSC amplitude in cultured neurons (Figure 2A). This increase was blocked by addition of citral (Figure 2A). Moreover, we blocked RA synthesis with 4-(diethylamino)-benzaldehyde (DEAB), an inhibitor of retinal dehydrogenase (RALDH) (Russo et al., 1988), the enzyme that catalyzes the next step oxidation from ROLDH and converts all-trans-retinal into RA. Similar to citral, DEAB completely blocked synaptic scaling induced by activity blockade (Figure 2B). These results suggest that RA synthesis is required for activity blockade-induced synaptic scaling.

If activity blockade-induced synaptic scaling is mediated by RA signaling, it should occlude further scaling effects induced by direct RA treatment. In both hippocampal slice and primary cultures, the homeostatic increase in synaptic strength induced by blocking neuronal activity with TTX and APV for 24 hours, as manifested in a significant increase in mEPSC amplitude in pyramidal neurons, occludes the subsequent action of RA treatment (1 μM, 2 hours for slice cultures, 30 minutes for primary cultures) (Figures 2C and D). Taken together, these data strongly suggest that RA is critically involved in homeostatic synaptic plasticity.

Blocking neuronal activity increases RA synthesis

The intriguing possibility that activity blockade-induced synaptic scaling is mediated by RA signaling led us to examine whether RA synthesis can be regulated in an activity-dependent manner. Retinoids are stored intracellularly as retinyl ester, which are converted to retinol when needed. Retinol is then metabolized to RA (Lane and Bailey, 2005). The oxidation that directly generates RA from retinal is catalyzed by retinal dehydrogenases (RALDHs) (Figure 3A). High levels of RALDH1 mRNA and protein are detected in fully differentiated hippocampal neurons, indicating that RA can be directly synthesized in neurons (Figure 3A and S2) (Wagner et al., 2002). To examine whether activity blockade enhances RA levels in neurons, we employed a retinoic acid response element (RARE)-based reporter system that

has been widely used *in vivo* and *in vitro* to detect RA (Suzuki et al., 2006; Thompson Haskell et al., 2002; Wagner et al., 1992). We generated a reporter construct containing three copies of the DR5 variant of the retinoic acid response element (direct repeat with 5 bp of spacing) and a GFP reporter gene (3xDR5-RARE-GFP) to monitor RA production in cultured neurons (Figure 3B). The detection system was validated in HEK293 cells in which direct RA treatment induced a robust increase in GFP when transiently transfected with the 3xDR5-RARE-GFP reporter (Figures S3A and B).

We transfected neurons at 13 DIV with 3xDR5-RARE-GFP, and examined the GFP fluorescence intensity after six hours. Compared to the untreated condition, treatment with TTX and APV for 24 hours dramatically increased the expression of the GFP reporter, while a control GFP construct lacking the RARE regulatory sequence showed no change in expression (Figures 3C and D). Interestingly, blocking neuronal activity with TTX alone for 24 hours, a protocol that induces a mechanistically distinct form of synaptic scaling (Sutton et al., 2006), did not yield a significant increase in the GFP reporter expression (Figure 3C and D).

To further validate that the increased GFP reporter expression reflects synthesis of RA in neurons, we examined the effect of the RA synthesis blocker DEAB on reporter expression. DEAB, added to the neurons together with TTX and APV, reduced the GFP-reporter signal in a dose-dependent manner (Figure 3C and E). At a concentration of 10 μM, which blocked synaptic scaling induced by TTX+APV (Figure 2B), DEAB completely blocked RA synthesis, as indicated by a lack of significant increase in reporter expression (Figure 3E). It is worth noting that even with the highest DEAB concentration (100 μM), which presumably completely blocked RA synthesis, the GFP reporter expression levels were comparable to those found in mock-treated neurons, indicating that at basal conditions (no activity blockade), the ambient RA level in neurons is very low.

To rule out the possibility that the observed increase in the GFP reporter expression was caused by activity-dependent changes in the neuron's general transcriptional and/or translational activity acting on the reporter, and to directly test whether RA can act as a diffusible signal acting on neighboring cells (i.e., function in a cell non-autonomous manner), we repeated the RA detection experiment using HEK293 cells transfected with the 3xDR5-RARE-GFP reporter. An hour after transfection, HEK293 cells were co-plated with neurons. A significant increase in GFP expression in the HEK293 cells was observed as early as eight hours after the onset of TTX and APV treatment in comparison to the mock-treated group, and the difference was retained 24 hours after onset of the activity blockade (Figures 3F and G). Treating HEK293 cells directly with TTX+APV for 24 hours did not affect 3xDR5-RARE-GFP reporter expression (Figure S4A). In addition, a control GFP construct lacking the RARE sequence did not show expression differences under these conditions (Figures 3G). Although the HEK293 cells plated directly on neurons were able to detect increased RA levels in TTX- and APV-treated neurons, conditioned media collected from neuronal cultures that had been treated with TTX and APV for 24 hours did not increase 3xDR5-RARE-GFP reporter expression in HEK293 cells (Figure S4B). The lack of free RA in the conditioned media was probably due to its lipophilic and labile nature.

Taken together, these results demonstrate that blocking neuronal activity by the TTX and APV treatment strongly increases RA levels in neurons, and that RA acts locally in these neurons and in surrounding cells.

RA promotes surface expression of GluR1-containing AMPA receptors

The selective increase of mEPSC amplitude but not frequency by RA treatment, and the lack of an effect of RA on spine density, suggest that RA acts postsynaptically to enhance

synaptic strength in existing synapses. To examine whether RA increases synaptic transmission by increasing postsynaptic AMPA-receptor function, we stained the cell surface of neurons treated with DMSO (vehicle) or 1 μM RA for surface-expressed GluR1 and GluR2 AMPA-receptor subunits (Figures 4A). Indeed, RA significantly increased the surface levels of GluR1, but not of GluR2 (Figure 4B).

We also examined surface GluR1 expression levels with surface protein biotinylation. Either RA or TTX + APV treatment alone significantly increased the surface GluR1 level (Figures 4C and D). However, application of both treatments together did not produce additional enhancement (Figures 4C and D), consistent with our electrophysiological results demonstrating that activity blockade-induced synaptic scaling occludes RA-induced increase in synaptic transmission (Figures 2C and D).

The selective increase in GluR1 surface expression by RA suggests that homomeric GluR1 receptors are inserted during RA-induced synaptic scaling. Activity blockade-induced synaptic scaling is mediated by homomeric GluR1 receptors, and can be blocked by philanthotoxin-433 (PhTx), a blocker of homomeric AMPA-receptors lacking the GluR2 subunit (Ju et al., 2004; Shepherd et al., 2006; Sutton et al., 2006; Thiagarajan et al., 2005). Indeed, the RA-induced increase in mEPSC amplitude was reversed by bath application of 5 μM PhTx in dissociated cultures (Figures 4E and F) and in hippocampal slice cultures (Figure 4G), indicating that RA-induced synaptic insertion of homomeric GluR1 receptors is responsible for the observed scaling effect. In contrast, basal synaptic transmission was not affected by PhTx (Figure S5), which is consistent with the notion that AMPA receptors supporting basal synaptic transmission are GluR2-containing heteromeric receptors.

RA induces transcription-independent local translation of GluR1 in dendrites

Activity blockade-induced, in particular, TTX and APV-induced synaptic scaling requires dendritic protein translation (Ju et al., 2004; Sutton et al., 2006; Sutton et al., 2004). GluR1 mRNA is found in neuronal dendrites, and is believed to be translated locally (Grooms et al., 2006; Miyashiro et al., 1994; Poon et al., 2006). To test whether RA induces an increase in postsynaptic GluR1, we investigated whether RA-induced synaptic scaling depends on gene transcription or translation. The protein synthesis inhibitor anisomycin (40 μM) blocked the RA-induced increase in mEPSC amplitude in both hippocampal slice cultures (Figure 5A) and dissociated cultures (Figures 5B). Moreover, the increase in surface GluR1 expression by RA treatment was also completely prevented by anisomycin or cycloheximide (100 μM; see Figure 5C). By contrast, the transcription inhibitor actinomycin D (50 μM) failed to block the effects of RA on mEPSC amplitude or on surface GluR1 expression (Figures 5A, B and C). Thus, RA regulates synaptic transmission by a novel translation-dependent, but transcriptionin-dependent mechanism.

Combining *in situ* hybridization and immunocytochemistry, we found that GluR1 mRNA was present in neuronal dendrites (Figure 6A), consistent with previous reports (Grooms et al., 2006). We next examined RA-induced local translation of GluR1 in synaptoneurosomes isolated from 3–4 week old rat hippocampi. The synaptoneurosome preparation was enriched in synaptic proteins such as GluR1, PSD-95, and free of nuclear proteins such as histone protein H3 (Figure 6B). Brief treatment of synaptoneurosomes with 1 or 10 failed to block the effects of RA M RA for 10 minutes at 37 °C specifically increased GluR1 protein level (Figure 6C), but not other synaptic proteins such as GluR2 and PSD-95 (Figure 6D). Consistent with our results obtained from cultured neurons and characteristic of local protein translation, the RA-induced increase in GluR1 synthesis in synaptoneurosomes was blocked by the protein synthesis inhibitors anisomycin and cycloheximide, but was not affected by transcription inhibitor actinomycin D (Figure 6E). Taken together, these results indicate that

RA acts in neuronal dendrites to activate local translation of GluR1 protein in a transcription-independent manner.

Activity blockade- and RA-induced synaptic scaling is RARα-dependent

What molecule could be a potential mediator for this novel dendritic RA signaling we observed? Conventional retinoid signaling is mediated by two classes of nuclear receptors, the retinoic acid receptors (RARs) and the retinoid X receptors (RXRs), each of which has three isotypes α, β and γ All-trans RA selectively activates the RARs, but not RXRs. In hippocampal CA1–CA3 pyramidal cells, both the RARα transcript and RARα protein are detected at high levels (Krezel et al., 1999; Zetterstrom et al., 1999). Curiously, RARα was also present in synaptoneurosomes although its level was not changed by the RA treatment (Figure 6D). Immunohistochemistry staining in adult hippocampal slices further confirmed that RARα not only is found in the nucleus, but also is present in dendrites, evidenced by its colocalization with a somatodendritic marker MAP2 (Figure 6F).

To directly investigate whether RARα is required for synaptic scaling, we used a RARα shRNA construct to acutely knockdown RARα expression in hippocampal neurons. This method allows us to avoid confounding factors in the RARα-null mice, such as abnormal neuronal development and perinatal lethality (LaMantia, 1999; Lufkin et al., 1993; Mark et al., 1999). The RARα shRNA efficiently reduced RARα expression in heterologous cells and neurons after three days of expression (Figures S6 A and B). Knockdown of RARα in cultured neurons did not change basal synaptic transmission (Figures 7A–7C), surface GluR1 or GluR2 expression (Figure 7E), or spine density (Figure S7), suggesting that RARα does not contribute to the maintenance of basal level of synaptic AMPA receptors or spine morphogenesis. However, activity blockade-induced synaptic scaling and the increase in surface GluR1 level were both completely blocked (Figures 7A, B and E). This result was also validated in hippocampal neurons from cultured slices (Figure 7D). Surface GluR2 expression level remained unchanged under all conditions (Figure 7E). Co-expression with a rescue RARα construct resistant to shRNA (Figure S6A) completely restored the synaptic scaling induced by activity blockade in RARα shRNA-expressing neurons (Figure 7B). Similarly, RARα shRNA prevented the increase in mEPSC amplitude induced by direct RA treatment (Figure 7C).

Although our results indicate that RA, signaling through RARα, regulates local GluR1 synthesis in a transcription-independent manner, the possibility remains that the observed effects of RARα shRNA on synaptic scaling were due to undocumented genomic functions of RARα on the levels of GluR1 transcripts or translation factors in dendrites. However, the total GluR1 expression level in the neurons was not altered by RARα shRNA three days after the transfection (Figure S8A). In addition, dendritic GluR1 and CaMKIIα synthesis induced with a high-K^+ protocol (Gong et al., 2006; Ju et al., 2004) was as strong in RARα shRNA-transfected neurons as in control vector (pSuper)-transfected or neighboring untransfected neurons (Figures S8 A and B). These results rule out the possibility that RARα knockdown alters basal GluR1 transcription or affects the general dendritic protein translation machinery, suggesting that dendritic RARα signaling is selectively involved in synaptic scaling.

We next directly examined the effect of RARα activation on synaptic scaling using an RARα-selective agonist, AM580 (Liao et al., 2004). In primary cultured neurons, treatment of 1 or 10 μM AM580 induced a significant increase in mEPSC amplitude, which lasted for at least one hour after AM580 washout (Figures 8 A and B). Treatment with 1 μM AM580 also significantly increased the mEPSC amplitude of neurons from cultured hippocampal slices (Figures 8C and D). Similar to the action of RA in hippocampal synaptoneurosomes, which induced rapid synthesis of GluR1 protein (Figure 6C), treatment of hippocampal

synaptoneurosomes with AM580 for 10 minutes also induced a significant increase in the GluR1 level (Figures 8 E and F), suggesting that the RARα protein in dendrites indeed mediates local translation of GluR1. Taken together, these results demonstrate that RARα is both necessary and sufficient for synaptic scaling induced by activity blockade or RA treatment.

DISCUSSION

Different forms of homeostatic synaptic plasticity maintain the stability and coding capacity of neural circuits when neuronal activity levels are altered (Davis, 2006; Grunwald et al., 2004; Rich and Wenner, 2007; Turrigiano and Nelson, 2004). Homeostatic synaptic plasticity may manifest as altered pre-synaptic transmitter release, synaptic vesicle loading properties, postsynaptic receptor functions, or neuronal membrane properties (Davis, 2006; Rich and Wenner, 2007). In this study, we focused on a specific form of homeostatic synaptic plasticity induced by activity blockade with TTX and APV. Earlier studies indicate that during this form of homeostatic plasticity, blocking neuronal activity by TTX and APV induces rapid dendritic synthesis and synaptic insertion of AMPA-receptors (Ju et al., 2004; Sutton et al., 2006). Here we show that RA acts as a synaptic signal that mediates the increase in postsynaptic AMPA-receptor levels during this type of activity-blockade induced homeostatic plasticity, and that RA acts by regulating dendritic protein synthesis. This novel form of RA signaling requires dendritically localized RARα This conclusion is based on the following evidence:

1. Neuronal activity blockade by TTX and APV rapidly increases the production of endogenous RA in cultured neurons, suggesting that RA synthesis is regulated by synaptic activity. A different form of synaptic scaling that is induced by TTX treatment alone and does not involve local protein synthesis (Sutton et al., 2006), did not induce RA synthesis in neurons (Figure 3).
2. Application of exogenous RA directly increases glutamatergic synaptic transmission in a multiplicative manner that resembles synaptic scaling (Figures 1A–1F).
3. Activity blockade-induced synaptic scaling occludes the increase in synaptic transmission induced by RA (Figures 2C and 2D).
4. Blocking RA synthesis with the retinol dehydrogenase inhibitor citral or the retinal dehydrogenase inhibitor DEAB prevents expression of TTX and APV-blockade induced homeostatic plasticity, indicating that RA is required for this type of homeostatic plasticity (Figures 2A and 2B).
5. The RA-induced increase in synaptic transmission involves the stimulation of the synthesis and postsynaptic insertion of GluR1-type AMPA-receptors, but not of GluR2-type AMPA-receptors (Figure 4), as previously shown for activity blockade-induced homeostatic synaptic plasticity (Ju et al., 2004;Shepherd et al., 2006;Sutton et al., 2006;Thiagarajan et al., 2005).
6. Protein synthesis inhibitors block the RA-induced increase in synaptic transmission (Figures 5A and 5B), again as previously shown for activity blockade-induced homeostatic plasticity (Ju et al., 2004; Sutton et al., 2006). Protein synthesis inhibitors also block the specific synthesis and plasma membrane insertion of GluR1 receptors induced by RA (Figure 5C).
7. RA stimulates GluR1 synthesis and insertion even in synaptoneurosomes, a biochemical preparation that lacks nuclei, demonstrating that the postsynaptic

effect of RA operates by stimulating local protein synthesis (Figure 6) (Ju et al., 2004;Sutton et al., 2006).

8. The nuclear receptor RARα is also present in neuronal dendrites (Figures 6D and F). Knocking down RARα blocked both activity blockade-induced and RA-sinduced synaptic scaling (Figure 7).

9. Selective activation of RARα increases excitatory synaptic transmission and rapid synthesis of GluR1 in synaptoneurosomes (Figure 8).

It is important to note that for most of these observations, i.e., wherever possible, we confirmed the findings in two systems – cultured neurons and slices – to ensure that the findings are not a peculiarity of dissociated cultured neurons.

The identification of RA as a signaling molecule in homeostatic plasticity has important implications. RA may act cell-autonomously and as a local diffusible molecule during synaptic scaling. Our observation that RARE reporter-expressing HEK cells co-cultured with neurons are able to detect increased RA synthesis demonstrates that RA acts, at least in part, non cell-autonomously, and supports the notion that RA acts as a short-range diffusible molecule.

Unlike input-specific synaptic plasticity (i.e., LTP and LTD), homeostatic synaptic plasticity is generally believed to be triggered by a global change in neuronal activity that involves modification of all synapses (Thiagarajan et al., 2005; Turrigiano et al., 1998; Turrigiano and Nelson, 2004). Recently it has been shown, however, that local changes of activity in a segment of neuronal dendrite can also induce homeostatic compensation in a subset of synapses (Hou et al., 2008; Sutton et al., 2006). A diffusible signal such as RA facilitates the expression of homeostatic synaptic plasticity at multiple synapses of a neuron, and even of nearby neurons. On the other hand, because the RALDH protein is present throughout dendrites and axons, RA synthesis may be achieved locally and regulate a subset of synapses in the event of local homeostatic compensation. The notion that RA can be rapidly synthesized in an activity-dependent fashion extends the list of signaling molecules contributing to activity-dependent synaptic plasticity, although it remains to be determined how RA biosynthesis is regulated by neuronal activity.

Because RA is an important regulator of pattern formation in development and is necessary for the maintenance of epithelial tissues in adult animals (Lotan, 1995; Morriss-Kay and Sokolova, 1996), the activity of RA is tightly controlled in tissues through balancing the rate of RA synthesis and metabolism. A number of key enzymes and proteins involved in RA synthesis have been identified, including serum retinol binding protein, cellular retinol-binding proteins, ROLDH, RALDH and cellular retinoic acid-binding proteins. The final step in RA synthesis, which is the oxidation of retinal into RA catalyzed by RALDH, is considered a rate-limiting step of RA biogenesis (Blomhoff et al., 1991). The expression of RALDH is developmentally controlled, and further regulated by hormones and cholesterol metabolites (Huq et al., 2006; Ruhl et al., 2006). Changes in neuronal activity may modulate RA synthesis by altering RALDH expression in neurons. In addition to RALDH activity, RA synthesis can be regulated by the availability of retinol, which is stored intracellularly as retinyl ester, a reaction catalyzed by lethicine:retinol acyltransferase (Lane and Bailey, 2005). Sequestration of retinol as retinyl ester limits RA synthesis, and blocking retinyl ester formation by reducing lethicine:retinol acyltransferase activity increases RA levels (Isken et al., 2007). Understanding how neuronal activity modulates the expression level of various enzymes in RA synthesis will shed light on the mechanism by which neurons homeostatically maintain their activity through regulating RA availability.

In addition to retinoids, other molecular players such as the immediate-early gene Arc/Arg3.1, CaMKIIα and β, TGF-β and glia cell-derived TNFα have also been implicated in homeostatic synaptic plasticity (Shepherd et al., 2006; Stellwagen and Malenka, 2006; Sweeney and Davis, 2002; Thiagarajan et al., 2002) (Figure 9). RA differs from these molecules, however, in that it is the first molecule shown to regulate dendritic protein synthesis during homeostatic plasticity. The potential interplay between these various signaling molecules may have implications in the mechanisms involved at different stages of homeostatic plasticity that require translational or transcriptional events. For example, RA has been shown to regulate TNFα transcription (Dheen et al., 2005; Nozaki et al., 2006), suggesting the exciting possibility that neuronal and glial signaling pathways interact in homeostatic plasticity. In addition to homeostatic plasticity, Arc/Arg3.1, CaMKIIα and RA signaling are also involved in LTP and/or LTD (Chiang et al., 1998; Cocco et al., 2002; Lisman et al., 2002; Misner et al., 2001; Plath et al., 2006). These signaling molecules may be components of common mechanisms for multiple forms of synaptic plasticity, rather than specific players for synaptic scaling. The versatility of RA signaling in regulating transcription and translation independently in both developing and adult brain further suggests the possibility that different types of synaptic plasticity may interact functionally. The molecular players of homeostatic plasticity are just beginning to be uncovered. A major question arises as how RA achieves this astonishing effect in synaptic scaling. The results of our study provide preliminary evidence that RARα a known nuclear receptor that regulates transcription, is also involved in translational regulation in neuronal dendrites. It remains to be determined how RARα achieves this novel regulation in dendrites. RARα protein is found to translocate into dendritic RNA granules upon translational activation (Maghsoodi and Chen, unpublished observations). Further studies will be required to delineate the interactions between these different signaling pathways in homeostatic and other forms of synaptic plasticity.

EXPERIMENTAL PROCEDURES

DNA Constructs

To make the 3xDR5-RARE-EGFP reporter construct, three copies of the DR5 retinoic acid response elements (de The et al., 1990) were inserted end-to-end into the AseI and BglII sites of pEGFP-N1 (Clontech, Mountain View, CA), which also removed the pre-existing CMV promoter. A thymidine kinase promoter from pBS-DR5-RARE (gift from Anthony LaMantia) was then inserted downstream of the 3xRARE into the multiple cloning site using HindIII and PstI.

Rat RARα-GFP was amplified from rat hippocampal cDNA using the following primers: RARα F, 5’-atatctcgagatgtacgaaagtgtagaagtc-3’; and RARα R, 5’-atatgaattcgtggggattgagtggctgggct-3’, and inserted into XhoI/EcoRI restriction sites of pEGFP-N1 (Clontech, Mountain View, CA).

All siRNA constructs were inserted into pSUPER-Retro GFP (Oligogene, Seattle, WA) according to the manufacturer’s protocol. RARα siRNA was directed against bases 370–388 of rat RARα (NM_031528). The sense sequence was as follows: 5’-gacaagaactgcatcatca-3’ and the antisense sequence was: 5’-tgatgatgcagttcttgtc-3’. To generate siRNA resistant RARα, PCR-based site mutagenesis was used to induce a silent mutation at base 378 (C-T).

Antibodies

The following mouse monoclonal primary antibodies were used in this study: actin (Chemicon, Temecula, CA), FMRP (Chemicon), GluR2 (Chemicon), MAP2 (Abcam), PSD95 (Affinity Bioreagents, Golden, CO), Flag (Sigma). The following rabbit polyclonal

primary antibodies were used: GFP (Abcam), RALDH1 (Abcam), GluR1 (Oncogene-Calbiochem, San Diego, CA), GluR1 (Upstate, Charlottesville, VA), GluR2 (Chemicon), Histone, H3 CT (Upstate), RARα (Santa Cruz Biotechnologies, Santa Cruz, CA). The following secondary antibodies from Jackson Immuno Research (West Grove, PA) were used: anti-mouse Cy2, anti-rabbit Cy2, anti-mouse Cy3, anti-rabbit Cy3.

Drugs and chemicals

The following drugs and chemicals were purchased from Sigma Aldrich: all-trans retinoic acid, philanthotoxin-433, anisomycin, actinomycin D, cycloheximide, and picrotoxin. Tetrodotoxin was purchased from Tocris Biosciences (Ellisville, MO), D-APV from Fisher. AM580 was from Biomol International, LP (Plymouth Meeting, PA).

Cell Cultures, transfection, drug treatment and immunolabeling

Primary hippocampal cultures were prepared from the brains of rats at embryonic day 22 and maintained in serum-free Neurobasal medium supplemented with B-27 and Glutamax (Gibco-Brl, Grand Island, NY) for two weeks *in vitro*(Nam and Chen, 2005). Hippocampal slice cultures were prepared from 7–8 days old rat pups (Schnell et al., 2002) and maintained in Neurobasal-A medium supplemented with horse serum (Hyclone, Logan, UT), insulin (Sigma) and Glutamax. Human embryonic kidney (HEK)-293 cells were cultured in Dulbecco's modified Eagles medium (DMEM) supplemented with 10% fetal bovine serum (Gibco-Brl). Neurons were transfected using Lipofectamine 2000 (Invitrogen, Carlsbad, CA) with a protocol described previously (Nam and Chen, 2005). HEK293 cells were transfected using HEKfectin (BioRad, Hercules, CA) according to the manufacturer's instructions. Stock solutions of all–trans-RA in DMSO were freshly made right before treatment and the final concentration of DMSO in culture media is 0.05% or lower. Twenty-four-hour treatment of 1 μM TTX and 100 μM APV was used to induce synaptic scaling in dissociated cultures and thirty-six-hour treatment of 10 μM TTX and 1 mM APV was used to induce synaptic scaling in slice cultures. Immunocytochemistry was performed on cultures fixed with 2% paraformaldehyde (15min, room temperature) and washed with PBS containing 0.3% Triton X100 before incubation with primary and secondary antibodies.

RA synthesis inhibitor treatment

A stock solution of 5mM Citral (Sigma-Aldrich) was prepared in DMSO. Neurons were treated with 5μM Citral, TTX, and APV for 24 hours prior to electrophysiological recording. A stock solution of 1M 4-diethylamino-benzaldehyde (DEAB; Sigma-Aldrich) was prepared in DMSO. Serial dilutions generated stocks of DEAB at concentrations of 100mM, 10mM, 1mM, 0.1mM, and 0.01mM. Neurons were treated (1:1000) with each concentration of DEAB coincided with the onset of activity blockade and continued for 24 hours.

Lentivirus shRNA Transfer Vector and Lentivirus Production

Human U6 (Dr. John Rossi, City of Hope) was amplified from pBS-U6 using the following primers: U6 BamHI F, 5'-ataagaatgcggccgccccggggatccaaggtcggg-3' and U6 RARα shRNA XbaI R, 5'-gctctagaaaaagacaagaactgcatcatcatctcttgaatgatgatgcagttcttgtcggtgtttcgtcctttccac-3' and cloned into pBS (Stratagene). The U6-RARα shRNA product was then subcloned into HIV U6 GFP-fill CMV-Neo (HU6G-fill CN) (a generous gift from Dr. David Schaffer, UC Berkeley) to generate HU6RARα CN. The human synapsin (hSYN)-EGFP cassette then replaced the CMV-Neo cassette to form HU6RARα-SG.

Lentivirus was produced as described (34). Briefly, human embryonic kidney 293T cells were transfected using the calcium phosphate method with the transfer vector and three helper plasmids, pRSV-REV, pIVS-vesicular stomatitis G protein (VSVg), and pMDL gag/

pol at 22.5, 14.7, 8, and 5.7 μg of DNA per 15-cm plate. After 48 hours, the supernatants of eight plates were pooled, spun at 2000 rpm for 5 min, passed through a 0.45 μm filter, spun at 25,000 rpm through a sucrose cushion for 1.5 h, the pellets were pooled and spun at 24,800 rpm for 1.5 hr before being resuspended in 100 μl PBS.

Electrophysiology

Whole-cell patch-clamp recordings were made at room temperature from 14–15 DIV cultured neurons, with 4–6 MΩ; patch pipettes filled with an internal solution containing (in mM) 120 CsCl, 2 $MgCl_2$, 5 EGTA, 10 HEPES, 0.3 Na_3-GTP, 4 Na_2-ATP, pH 7.35. Cultures were continuously superfused with external solution (in mM, 100 NaCl, 26 $NaHCO_3$, 2.5 KCl, 11 glucose, 2.5 $CaCl_2$, 1.3 $MgSO_4$, 1.0 NaH_2PO_4). Patch-clamp recordings from slice cultures were also made at room temperature from 6–8 DIV slices with a 4–6 MΩ patch pipettes filled with an internal solution containing (in mM) 140 CsCl, 2 $MgCl_2$, 5 EGTA, 10 HEPES, 0.3 Na_3-GTP, 4 Na_2-ATP, pH 7.35. Slices were continuously superfused with external solution (in mM, 120 NaCl, 26 $NaHCO_3$, 2.5 KCl, 11 glucose, 2.5 $CaCl_2$, 1.3 $MgSO_4$, 1.0 NaH_2PO_4). For mEPSC recording, tetrodotoxin (1 μM) and picrotoxin (100 μM) were included in the external saline. Cells were held at -60 mV. For PhTx recordings, 5 μM PhTx or vehicle control was bath-perfused for ten minutes before recording. Miniature responses were analyzed with Mini Analysis Program from Synaptosoft.

AMPA receptor surface labeling using immunocytochemistry

Cultured hippocampal neurons (14–15 DIV) were treated with 1 μM RA or 1 μM TTX and 100 μM APV prior to surface labeling of AMPA receptors. Cultures were washed with PBS containing 1 mM $CaCl_2$ and 0.5 mM $MgCl_2$ (PBS/Ca^{2+}/Mg^{2+}) with 4% sucrose. Neurons were pre-incubated at 37°C for 10 minutes with primary antibodies against GluR1 or GluR2 to allow labeling of surface AMPA receptors, and washed in ice-cold PBS/Ca^{2+}/Mg^{2+}. After fixation with 4 % PFA+4 % sucrose, cells were blocked using a detergent-free blocking solution (PBS with 2% normal goat serum, 0.02% sodium azide) for 1 hr, followed by secondary antibody incubation at room temp for 1 hr.

Surface biotinylation assay

Cultured hippocampal cells were washed four times with cold PBS/Mg^{2+}/Ca^{2+}, and surface proteins were biotinylated with 1 mg/ml Ez-link sulfo-NHS-SS-biotin (Pierce, Madison, WI) in ice cold PBS/Ca^{2+}/Mg^{2+} for 20 min at 4°C. Cells were washed with 0.1 M glycine in ice cold PBS/Ca^{2+}/Mg^{2+} to stop further biotinylation of the surface protein. After four more washes with ice cold PBS, cells were collected using centrifugation. Biotinylated cells were solubilized with lysis buffer (PBS with 1% triton-X, 1% NP-40, 10% glycerol, 25 mM $MgCl_2$ and a protease inhibitor cocktail). Lysates were centrifuged to remove cell debris and nuclei at 14000 rpm for 30 min. Pre-cleared lysate was bound over night at 4°C using Ultralink-immobilized streptavidin beads to precipitate biotinylated proteins. Non-biotinylated proteins were removed by centrifugation at 1000 rpm for 3 min, and the beads were washed three times with lysis buffer. Biotinylated surface proteins were eluted with denaturing buffer at 75°C. Surface expressed AMPA receptors were detected by Western blot analysis.

siRNA Efficiency

Twenty-four hours prior to transfection, 5×10^5 HEK293 cells per well were seeded in 6-well plates (BD). To confirm RNAi efficacy, siRNA constructs were co-transfected with appropriate target contructs in a 3:1 ratio. Twenty-four hours after the transfection, cells were lysed in lysis buffer (50 mM Tris [pH 7.5], 150 mM NaCl, 5 mM EDTA, 1% Triton X-100, 10 μg/ml aprotinin, 1 mM PMSF) at a concentration of 2×10^4 cells/μl. The lysates

were then passed through a 25 1/2 G needle and run on 10% SDS polyacrylamide gels. Proteins were transferred to Immobilon-P PVDF membranes (Millipore), incubated in TBST (0.2%) with 5% non-fat milk for 1 hr, and immunoblotted as per standard protocols. Detection used a HRP secondary followed by Enhanced Chemiluminescence (Pierce, Rockford, IL).

KCl-induced local translation

Neurons were transfected with pSUPER or RARα siRNA for four days prior to KCl treatment. Briefly, neurons plated on glass coverslips were dipped once into a high-K^+ solution (12.5 mM NaCl, 90 mM KCl, 2.6 mM $MgSO_4$, 1 mM NaH2PO_4, 26.2 mM $NaHCO_3$, 11 mM Glucose, 10 μM Glycine, 2.5 mM $CaCl_2$) for 1 s followed by 10 s in a 2.5 mM KCl $NaHCO_3$-buffered solution. This was repeated three times at room temperature before the neurons were allowed to recover for 10 min at 37°C. Following the 10-minute incubation, the neurons were immediately fixed for immunocytochemistry.

Immunocytochemistry in slice

Hippocampal slices (400-μm thickness) were fixed in 4% paraformaldehyde for 1 hr, rinsed three times with PBS, then permeabilized with 0.5% Triton-X 100 for 1 hr, and rinsed three times with PBS again. Slices were then treated with 50 mM NH_4Cl for 20 minutes at room temperature, rinsed three times with PBS and blocked in 10% normal goat serum for 1 hr. Slices were subsequently incubated with RARα and MAP2 antibodies for 18 hrs at 4°C, followed by three one-hour washes in PBS. Cy2-conjugated goat anti-mouse and Cy3-conjugated goat anti-rabbit secondary antibodies were then applied for 18 hours at 4°C, followed by five one-hour PBS washes.

Image acquisition and quantification

For fluorescent image analysis, cells were chosen randomly from three or more independent batches of cultures with four or more cover slips per batch for each construct. Fluorescent images were acquired at room temperature with an Olympus FV1000 BX61WI laser scanning confocal microscope, using an Olympus Plan Apochromat 60x oil objective (N.A. 1.42, WD 0.15) or an Olympus U-Plan Apochromat 100X oil objective (N.A. 1.40, WD 0.12) with sequential acquisition setting at 1,024 × 1,024 pixel resolutions. Laser power and photomultipliers were set such that no detectable bleed-through occurred between different channels. Digital images of the cells were captured with FV1000 Imaging software (Olympus). Eight to ten sections were taken from top to bottom of the specimen, and brightest point projections were made. Images for the same experiments were taken using identical settings for laser power, photomultiplier gain and offset. These settings were chosen such that the pixel intensities for the brightest samples were just below saturation, except that when contours of the cell or contours of the neuronal processes had to be clearly determined, signals from certain areas (center of the HEK cell body or soma of the neurons) were saturated in order to obtain clear perimeter of the cell body or neuronal dendrites. Quantification of fluorescent signals of immunostained proteins was performed as described (Nam and Chen, 2005). Briefly, images collected using the same confocal settings were thresholded identically by intensity to exclude the diffuse/intracellular pool, and puncta were quantified by counting the number of supra-threshold areas of sizes between 0.25 and 4 $μm^2$. Results were averaged for at least 15 images per condition and the mean and standard error were calculated. Image quantification was performed by experienced investigators who were “blind” to the experimental conditions.

Synaptoneurosome preparation

Hippocampi from P15–P21 Sprague-Dawley rats were dissected and gently homogenized in a solution containing 33% sucrose, 10 mM HEPES, 0.5 mM EGTA, pH 7.4 and protease inhibitors. Nuclei and other debris were pelleted at 2000g for 5 minutes at 4°C and the supernatant filtered through 3 layers of 100-μm pore nylon mesh (Millipore, Bedford, MA), and a 5-μm pore PVDF syringe filter (Millipore, Bedford, MA). The filtrate was then centrifuged for 10 minutes at 10,000g at 4°C, and the supernatant removed. The synaptoneurosome-containing pellet was then resuspended in the appropriate amount of Minimum Essential Media (Invitrogen, Carlsbad, CA) containing protease and RNAsin (Amersham, Piscataway, NJ). Equal volumes were then aliquoted into opaque microfuge tubes. Appropriate samples were pretreated for 30 minutes at 37°C with 50 μM actinomycin D (Sigma, St Louis, MO), 100 μM cycloheximide (Sigma, St Louis, MO) or 40 μM anisomycin (Sigma, St Louis, MO). Appropriate concentrations (100 nM, 1 uM or 10 uM) of retinoic acid (Sigma, St Louis, MO) or AM580 was added to the samples, which were incubated for 10 minutes at 37°C, and immediately frozen in dry ice afterward.

In situ hybridization

14 DIV hippocampal neurons were fixed with 4% paraformaldehyde, permeabilized with 0.5% Triton X-100 for 5 minutes, and incubated in DEPC PBS containing 0.1% active DEPC for 15 minutes. Cells were then prehybridized with Rapid-Hyb buffer (Amersham Biosciences, Piscataway, NJ) in 50% formamide containing 0.1% Blocking Reagent (Roche, Indianapolis, IN) at 54°C. Hybridizations were performed at 54°C, and washes at 50°C in 1x SSC containing 50% formamide. Cells were co-incubated with an HRP-linked DIG antibody and rabbit polyclonal MAP2 antibody for one hour at room temperature, and then processed for tyramide signal amplification using a Cy3-TSA kit (Perkin-Elmer, Wellesley, MA). MAP2 was detected using Cy5-conjugated goat anti-mouse antibody. Digoxygenin-labeled GluR1 riboprobes were transcribed from PCR product T3 and T7 RNA polymerase site adapters. The forward primer used was 5’ T3-CAATCACAGGAACATGCGGC 3’ and the reverse primer 5’ T7-TCTCTGCGGCTGTATCCAAG 3’.

Statistical analysis

Single-factor ANOVA was used for statistical analysis. Values are presented as mean +/− s.e.m in the figures.

Supplementary Material

Refer to Web version on PubMed Central for supplementary material.

REFERENCES

Beattie EC, Stellwagen D, Morishita W, Bresnahan JC, Ha BK, Von Zastrow M, Beattie MS, Malenka RC. Control of synaptic strength by glial TNFalpha. Science 2002;295:2282–2285. [PubMed: 11910117]

Blomhoff R, Green MH, Green JB, Berg T, Norum KR. Vitamin A metabolism: new perspectives on absorption, transport, and storage. Physiol Rev 1991;71:951–990. [PubMed: 1924551]

Cassiday LA, Maher LJ 3rd. Having it both ways: transcription factors that bind DNA and RNA. Nucleic Acids Res 2002;30:4118–4126. [PubMed: 12364590]

Chen N, Napoli JL. All-trans-retinoic acid stimulates translation and induces spine formation in hippocampal neurons through a membrane-associated RARalpha. Faseb J 2008;22:236–245. [PubMed: 17712061]

Chiang MY, Misner D, Kempermann G, Schikorski T, Giguere V, Sucov HM, Gage FH, Stevens CF, Evans RM. An essential role for retinoid receptors RARbeta and RXRgamma in long-term potentiation and depression. Neuron 1998;21:1353–1361. [PubMed: 9883728]

Cocco S, Diaz G, Stancampiano R, Diana A, Carta M, Curreli R, Sarais L, Fadda F. Vitamin A deficiency produces spatial learning and memory impairment in rats. Neuroscience 2002;115:475–482. [PubMed: 12421614]

Davis GW. Homeostatic control of neural activity: from phenomenology to molecular design. Annu Rev Neurosci 2006;29:307–323. [PubMed: 16776588]

de The H, Vivanco-Ruiz MM, Tiollais P, Stunnenberg H, Dejean A. Identification of a retinoic acid responsive element in the retinoic acid receptor beta gene. Nature 1990;343:177–180. [PubMed: 2153268]

Dev S, Adler AJ, Edwards RB. Adult rabbit brain synthesizes retinoic acid. Brain Res 1993;632:325–328. [PubMed: 8149239]

Dheen ST, Jun Y, Yan Z, Tay SS, Ling EA. Retinoic acid inhibits expression of TNF-alpha and iNOS in activated rat microglia. Glia 2005;50:21–31. [PubMed: 15602748]

Di Renzo F, Broccia ML, Giavini E, Menegola E. Citral, an inhibitor of retinoic acid synthesis, attenuates the frequency and severity of branchial arch abnormalities induced by triazole-derivative fluconazole in rat embryos cultured in vitro. Reprod Toxicol. 2007

Echegoyen J, Neu A, Graber KD, Soltesz I. Homeostatic plasticity studied using in vivo hippocampal activity-blockade: synaptic scaling, intrinsic plasticity and age-dependence. PLoS ONE 2007;2:e700. [PubMed: 17684547]

Gong R, Park CS, Abbassi NR, Tang SJ. Roles of glutamate receptors and the mammalian target of rapamycin (mTOR) signaling pathway in activity-dependent dendritic protein synthesis in hippocampal neurons. J Biol Chem 2006;281:18802–18815. [PubMed: 16651266]

Grooms SY, Noh KM, Regis R, Bassell GJ, Bryan MK, Carroll RC, Zukin RS. Activity bidirectionally regulates AMPA receptor mRNA abundance in dendrites of hippocampal neurons. J Neurosci 2006;26:8339–8351. [PubMed: 16899729]

Grunwald ME, Mellem JE, Strutz N, Maricq AV, Kaplan JM. Clathrin-mediated endocytosis is required for compensatory regulation of GLR-1 glutamate receptors after activity blockade. Proc Natl Acad Sci U S A 2004;101:3190–3195. [PubMed: 14981253]

Guzowski JF, Timlin JA, Roysam B, McNaughton BL, Worley PF, Barnes CA. Mapping behaviorally relevant neural circuits with immediate-early gene expression. Curr Opin Neurobiol 2005;15:599–606. [PubMed: 16150584]

Hou Q, Zhang D, Jarzylo L, Huganir RL, Man HY. Homeostatic regulation of AMPA receptor expression at single hippocampal synapses. Proc Natl Acad Sci U S A 2008;105:775–780. [PubMed: 18174334]

Huq MD, Tsai NP, Gupta P, Wei LN. Regulation of retinal dehydrogenases and retinoic acid synthesis by cholesterol metabolites. Embo J 2006;25:3203–3213. [PubMed: 16763553]

Isken A, Holzschuh J, Lampert JM, Fischer L, Oberhauser V, Palczewski K, von Lintig J. Sequestration of retinyl esters is essential for retinoid signaling in the zebrafish embryo. J Biol Chem 2007;282:1144–1151. [PubMed: 17098734]

Ju W, Morishita W, Tsui J, Gaietta G, Deerinck TJ, Adams SR, Garner CC, Tsien RY, Ellisman MH, Malenka RC. Activity-dependent regulation of dendritic synthesis and trafficking of AMPA receptors. Nat Neurosci 2004;7:244–253. [PubMed: 14770185]

Kelleher RJ 3rd, Govindarajan A, Jung HY, Kang H, Tonegawa S. Translational control by MAPK signaling in long-term synaptic plasticity and memory. Cell 2004;116:467–479. [PubMed: 15016380]

Klann E, Dever TE. Biochemical mechanisms for translational regulation in synaptic plasticity. Nat Rev Neurosci 2004;5:931–942. [PubMed: 15550948]

Krezel W, Kastner P, Chambon P. Differential expression of retinoid receptors in the adult mouse central nervous system. Neuroscience 1999;89:1291–1300. [PubMed: 10362315]

Lal L, Li Y, Smith J, Sassano A, Uddin S, Parmar S, Tallman MS, Minucci S, Hay N, Platanias LC. Activation of the p70 S6 kinase by all-trans-retinoic acid in acute promyelocytic leukemia cells. Blood 2005;105:1669–1677. [PubMed: 15471950]

LaMantia AS. Forebrain induction, retinoic acid, and vulnerability to schizophrenia: insights from molecular and genetic analysis in developing mice. Biol Psychiatry 1999;46:19–30. [PubMed: 10394471]

Lane MA, Bailey SJ. Role of retinoid signalling in the adult brain. Prog Neurobiol 2005;75:275–293. [PubMed: 15882777]

Liao YP, Ho SY, Liou JC. Non-genomic regulation of transmitter release by retinoic acid at developing motoneurons in Xenopus cell culture. J Cell Sci 2004;117:2917–2924. [PubMed: 15161940]

Lin CH, Yeh SH, Lu KT, Leu TH, Chang WC, Gean PW. A role for the PI-3 kinase signaling pathway in fear conditioning and synaptic plasticity in the amygdala. Neuron 2001;31:841–851. [PubMed: 11567621]

Lisman J, Schulman H, Cline H. The molecular basis of CaMKII function in synaptic and behavioural memory. Nat Rev Neurosci 2002;3:175–190. [PubMed: 11994750]

Lotan RM. Squamous differentiation and retinoids. Cancer Treat Res 1995;74:43–72. [PubMed: 7779622]

Lufkin T, Lohnes D, Mark M, Dierich A, Gorry P, Gaub MP, LeMeur M, Chambon P. High postnatal lethality and testis degeneration in retinoic acid receptor alpha mutant mice. Proc Natl Acad Sci U S A 1993;90:7225–7229. [PubMed: 8394014]

Mark M, Ghyselinck NB, Wendling O, Dupe V, Mascrez B, Kastner P, Chambon P. A genetic dissection of the retinoid signalling pathway in the mouse. Proc Nutr Soc 1999;58:609–613. [PubMed: 10604193]

Misner DL, Jacobs S, Shimizu Y, de Urquiza AM, Solomin L, Perlmann T, De Luca LM, Stevens CF, Evans RM. Vitamin A deprivation results in reversible loss of hippocampal long-term synaptic plasticity. Proc Natl Acad Sci U S A 2001;98:11714–11719. [PubMed: 11553775]

Miyashiro K, Dichter M, Eberwine J. On the nature and differential distribution of mRNAs in hippocampal neurites: implications for neuronal functioning. Proc Natl Acad Sci U S A 1994;91:10800–10804. [PubMed: 7971965]

Morriss-Kay GM, Sokolova N. Embryonic development and pattern formation. Faseb J 1996;10:961–968. [PubMed: 8801178]

Nam CI, Chen L. Postsynaptic assembly induced by neurexin-neuroligin interaction and neurotransmitter. Proc Natl Acad Sci U S A 2005;102:6137–6142. [PubMed: 15837930]

Nozaki Y, Tamaki C, Yamagata T, Sugiyama M, Ikoma S, Kinoshita K, Funauchi M. All-trans-retinoic acid suppresses interferon-gamma and tumor necrosis factor-alpha; a possible therapeutic agent for rheumatoid arthritis. Rheumatol Int 2006;26:810–817. [PubMed: 16292516]

Plath N, Ohana O, Dammermann B, Errington ML, Schmitz D, Gross C, Mao X, Engelsberg A, Mahlke C, Welzl H, et al. Arc/Arg3.1 is essential for the consolidation of synaptic plasticity and memories. Neuron 2006;52:437–444. [PubMed: 17088210]

Poon MM, Choi SH, Jamieson CA, Geschwind DH, Martin KC. Identification of process-localized mRNAs from cultured rodent hippocampal neurons. J Neurosci 2006;26:13390–13399. [PubMed: 17182790]

Rich MM, Wenner P. Sensing and expressing homeostatic synaptic plasticity. Trends Neurosci 2007;30:119–125. [PubMed: 17267052]

Ruhl R, Fritzsche B, Vermot J, Niederreither K, Neumann U, Schmidt A, Schweigert FJ, Dolle P. Regulation of expression of the retinoic acid-synthesising enzymes retinaldehyde dehydrogenases in the uteri of ovariectomised mice after treatment with oestrogen, gestagen and their combination. Reprod Fertil Dev 2006;18:339–345. [PubMed: 16554009]

Russo JE, Hauguitz D, Hilton J. Inhibition of mouse cytosolic aldehyde dehydrogenase by 4-(diethylamino)benzaldehyde. Biochem Pharmacol 1988;37:1639–1642. [PubMed: 3358794]

Schnell E, Sizemore M, Karimzadegan S, Chen L, Bredt DS, Nicoll RA. Direct interactions between PSD-95 and stargazin control synaptic AMPA receptor number. Proc Natl Acad Sci U S A 2002;99:13902–13907. [PubMed: 12359873]

Schuman EM, Dynes JL, Steward O. Synaptic regulation of translation of dendritic mRNAs. J Neurosci 2006;26:7143–7146. [PubMed: 16822969]

Shepherd JD, Rumbaugh G, Wu J, Chowdhury S, Plath N, Kuhl D, Huganir RL, Worley PF. Arc/Arg3.1 mediates homeostatic synaptic scaling of AMPA receptors. Neuron 2006;52:475–484. [PubMed: 17088213]

Song Y, Hui JN, Fu KK, Richman JM. Control of retinoic acid synthesis and FGF expression in the nasal pit is required to pattern the craniofacial skeleton. Dev Biol 2004;276:313–329. [PubMed: 15581867]

Stellwagen D, Malenka RC. Synaptic scaling mediated by glial TNF-alpha. Nature 2006;440:1054–1059. [PubMed: 16547515]

Sutton MA, Ito HT, Cressy P, Kempf C, Woo JC, Schuman EM. Miniature neurotransmission stabilizes synaptic function via tonic suppression of local dendritic protein synthesis. Cell 2006;125:785–799. [PubMed: 16713568]

Sutton MA, Wall NR, Aakalu GN, Schuman EM. Regulation of dendritic protein synthesis by miniature synaptic events. Science 2004;304:1979–1983. [PubMed: 15218151]

Suzuki T, Nishimaki-Mogami T, Kawai H, Kobayashi T, Shinozaki Y, Sato Y, Hashimoto T, Asakawa Y, Inoue K, Ohno Y, et al. Screening of novel nuclear receptor agonists by a convenient reporter gene assay system using green fluorescent protein derivatives. Phytomedicine 2006;13:401–411. [PubMed: 16716909]

Sweeney ST, Davis GW. Unrestricted synaptic growth in spinster-a late endosomal protein implicated in TGF-beta-mediated synaptic growth regulation. Neuron 2002;36:403–416. [PubMed: 12408844]

Tanaka M, Tamura K, Ide H. Citral, an inhibitor of retinoic acid synthesis, modifies chick limb development. Dev Biol 1996;175:239–247. [PubMed: 8626029]

Thiagarajan TC, Lindskog M, Tsien RW. Adaptation to synaptic inactivity in hippocampal neurons. Neuron 2005;47:725–737. [PubMed: 16129401]

Thiagarajan TC, Piedras-Renteria ES, Tsien RW. alpha- and betaCaMKII. Inverse regulation by neuronal activity and opposing effects on synaptic strength. Neuron 2002;36:1103–1114. [PubMed: 12495625]

Thompson Haskell G, Maynard TM, Shatzmiller RA, Lamantia AS. Retinoic acid signaling at sites of plasticity in the mature central nervous system. J Comp Neurol 2002;452:228–241. [PubMed: 12353219]

Turrigiano GG, Leslie KR, Desai NS, Rutherford LC, Nelson SB. Activity-dependent scaling of quantal amplitude in neocortical neurons. Nature 1998;391:892–896. [PubMed: 9495341]

Turrigiano GG, Nelson SB. Homeostatic plasticity in the developing nervous system. Nat Rev Neurosci 2004;5:97–107. [PubMed: 14735113]

Wagner E, Luo T, Drager UC. Retinoic acid synthesis in the postnatal mouse brain marks distinct developmental stages and functional systems. Cereb Cortex 2002;12:1244–1253. [PubMed: 12427676]

Wagner M, Han B, Jessell TM. Regional differences in retinoid release from embryonic neural tissue detected by an in vitro reporter assay. Development 1992;116:55–66. [PubMed: 1483395]

Zetterstrom RH, Lindqvist E, Mata de Urquiza A, Tomac A, Eriksson U, Perlmann T, Olson L. Role of retinoids in the CNS: differential expression of retinoid binding proteins and receptors and evidence for presence of retinoic acid. Eur J Neurosci 1999;11:407–416. [PubMed: 10051741]

Acknowledgments

We thank Dr. Peng Jin (Emory University) for providing the FLAG-FMRP cDNA, Dr. Anthony Lamantia (University of North Carolina) for the RARE-TK vector, Drs. David Schaffer (UC Berkeley) and John Rossi (City of Hope) for the lentiviral vectors. We thank Marta Soden for helping with the slice culture preparation, Sandhiya Kalyanasundaram for technical assistance, and members of the Chen lab for discussion and comments on the manuscript. The work was supported by Mabel and Arnold Beckman Foundation, the David and Lucile Packard Foundation, the W. M. Keck Foundation, and NIMH (L.C.).

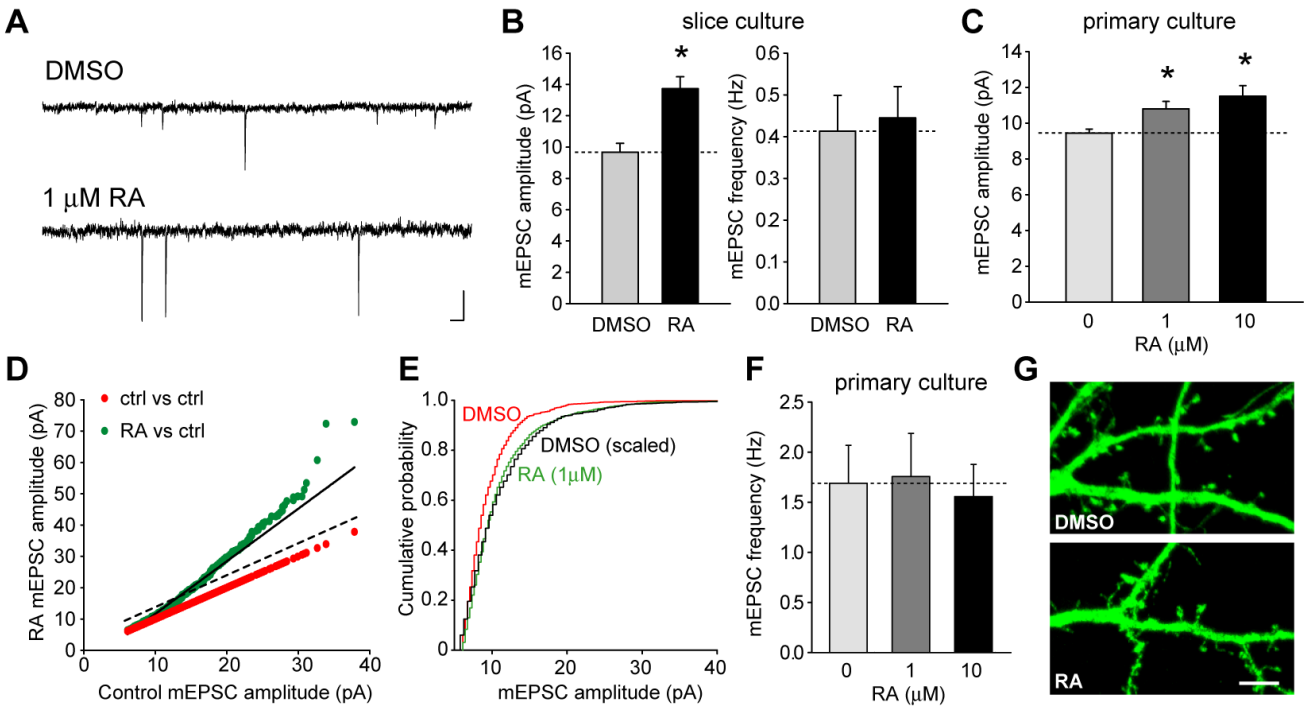

Figure 1. RA induces synaptic scaling

(A) Representative mEPSC traces from control (DMSO) and RA-treated neurons in dissociated cultures. Scale bar: 20 pA, 20 ms. (B) Acute RA (1 μM) treatment in cultured hippocampal slices significantly increased the amplitude but not frequency of mEPSCs in the pyramidal neurons (DMSO, n = 11; RA, n = 16; *, $p < 0.0005$). (C) RA treatment increased mEPSC amplitudes in dissociated neuronal cultures (n = 11 for each group; *, $p < 0.01$). (D) and (E) RA scaled up mEPSC amplitudes multiplicatively. (D) Ranked RA amplitudes were plotted against ranked control amplitudes (green dots), and the data is best described by a multiplicative (solid line), not an additive (dashed line), increase in mEPSC amplitudes. Red dots are control plotted against control, and have a slope of 1. Best fit: RA = control × 1.68 – 5.14, $R = 0.989$, $p < 0.0001$. (E) The cumulative distribution of mEPSC amplitudes from DMSO- (red) and RA (green)-treated neurons (n = 11 for each group). Scaling up the DMSO distribution by a factor of 1.68 produced a good fit to the RA-treated distribution (black line). (F) The average mEPSC frequency is not changed by RA treatment (n = 11 for each group, $p > 0.9$). (G) Acute RA treatment did not induce new spine formation. GFP-transfected neurons were treated with DMSO or 1 μM RA for one hour and fixed. No obvious morphological changes induced by RA were observed. Scale bar: 5 μm.

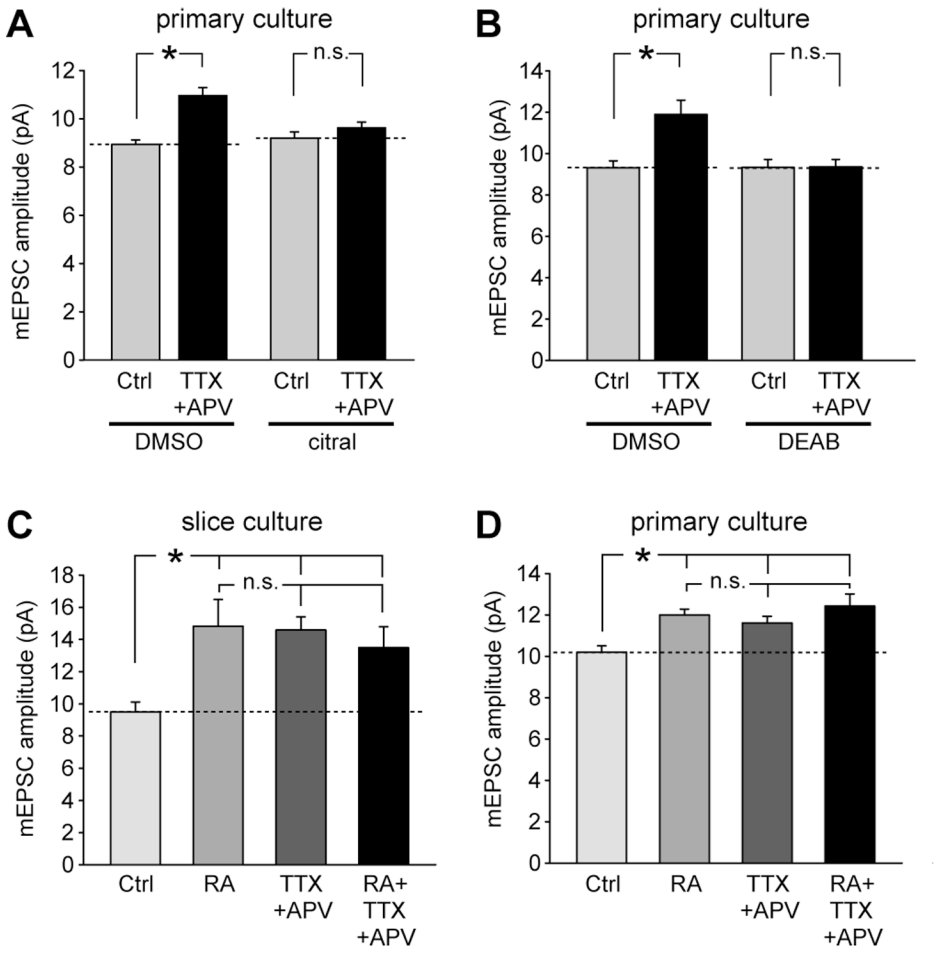

Figure 2. RA mediates activity blockade-induced synaptic scaling

(A) Citral, a ROLDH inhibitor, blocked TTX+APV-induced synaptic scaling. Neurons were treated with citral (5 μM) or DMSO together with TTX+APV for 24 hrs before electrophysiology recording. While TTX+APV alone induced synaptic scaling (n = 10 for each group, *, $p < 1 \times 10^{-4}$), no synaptic scaling was induced by activity blockade (n = 9 for each group, $p > 0.2$). (B) DEAB (10 μM), a RALDH inhibitor, also blocked TTX+APV-induced synaptic scaling (n = 11 for each group, *, $p < 0.005$; n.s., $p > 0.5$). (C) Blocking neuronal activity in cultured slices with TTX and APV induced synaptic scaling and occluded further increase by subsequent RA treatment (n = 10/group, *, $p < 0.005$). (D) Activity blockade-induced synaptic scaling occluded further RA-induced scaling in primary cultures (n = 10/group; *, $p < 0.01$).

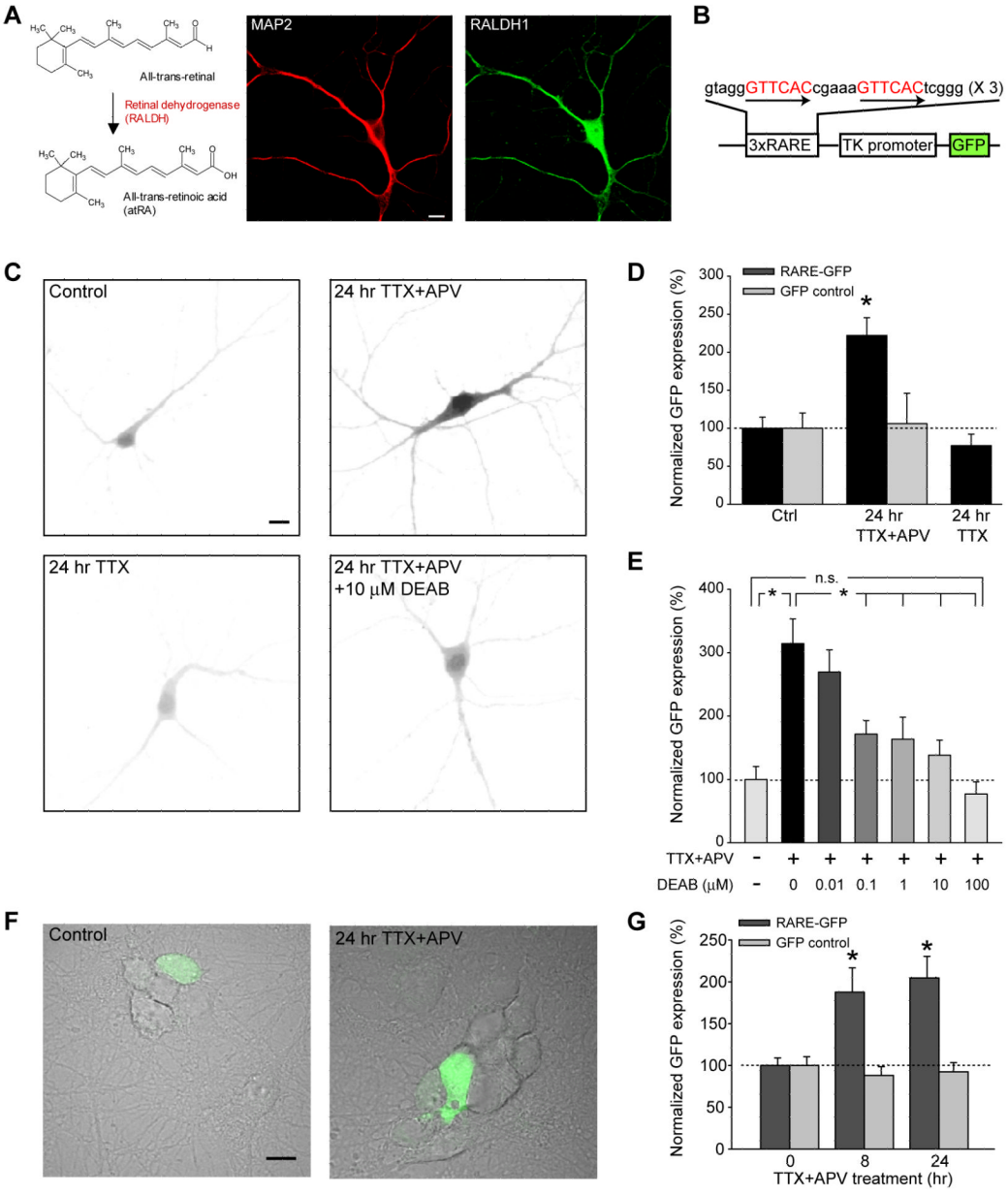

Figure 3. Activity blockade increases RA production in neurons

(A) RALDH1 expression in hippocampal neurons. 13 DIV hippocampal neurons showed strong immunoreactivity to RALDH1 (green). Neuronal dendrites and cell bodies are labeled with MAP2 antibody (red). Scale bar, 10 μm. (B) Schematics of the 3xDR5-RARE-GFP reporter construct. GFP reporter is driven by a thymidine kinase (TK) promoter. The transcription is regulated by an upstream RARE sequence consisting of 3 copies of DR5-RARE. (C) Example images of 3xDR5-RARE-GFP reporter expression in neurons under various treatment. Scale bar, 10 μm. (D) Activity blockade by TTX and APV for 24 hrs significantly increased 3xDR5-RARE-GFP reporter expression in neurons without changing control GFP expression (n = 10/group; *, $p < 1 \times 10^{-4}$, single factor ANOVA). TTX

treatment for 24 hours did not increase reporter expression ($n = 9$, $p > 0.3$). (E) DEAB blocked the increase in 3xDR5-RARE-GFP reporter expression by TTX+APV treatment in a dose-dependent manner ($n = 10$/group; *, $p < 0.0005$; n.s., $p > 0.4$). (F) and (G) Prolonged neuronal activity blockade (> 8 hrs) significantly increased GFP expression levels in co-plated HEK293 cells transfected with 3xDR5-RARE-GFP reporter without affecting control GFP expression ($n = 15$/group, *, $p < 0.01$). Scale bar, 10 μm. Single-factor ANOVA was used for all statistical analysis. Error bars represent SEM.

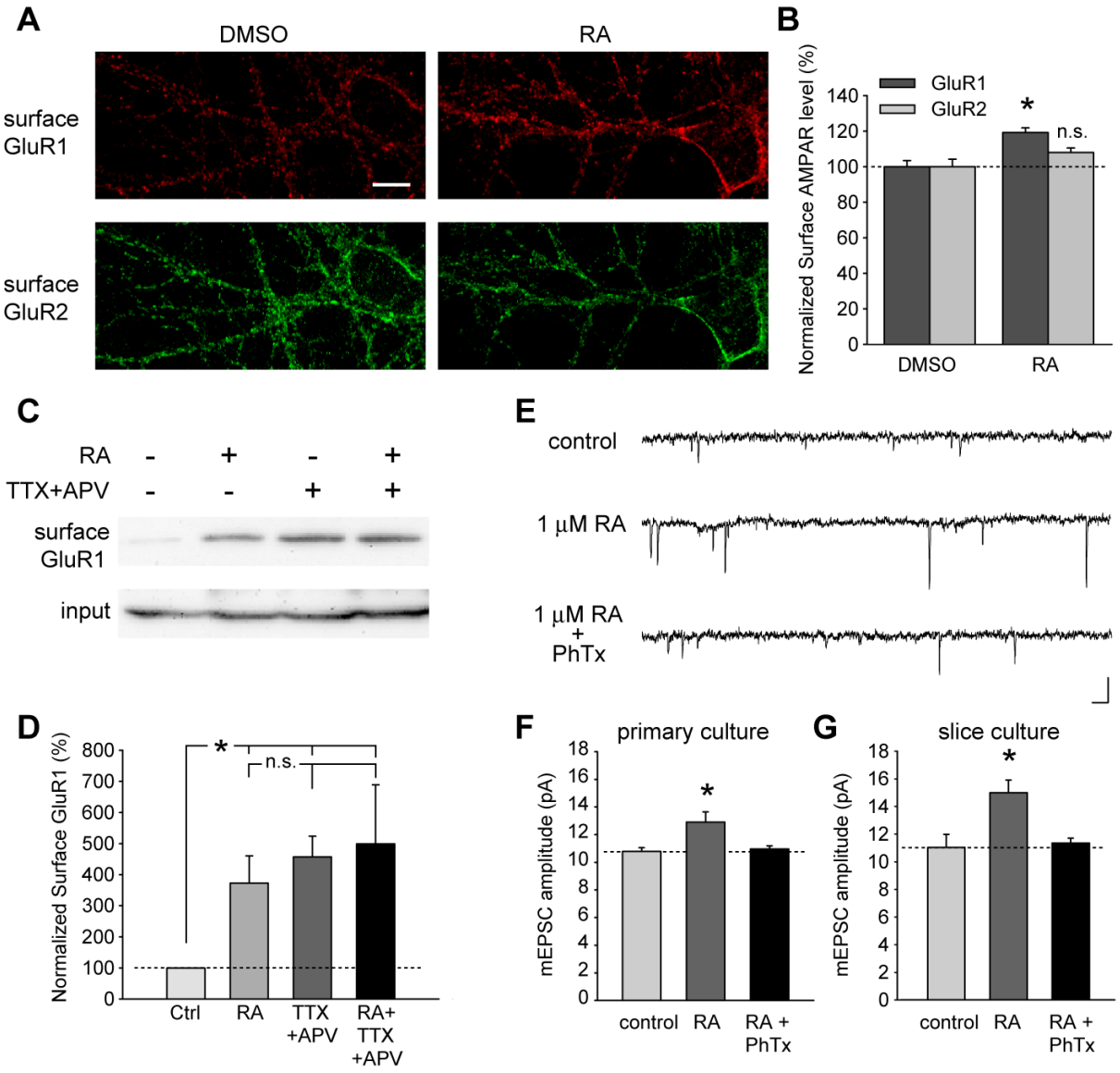

Figure 4. RA increased surface delivery of homomeric GluR1 receptors

(A) Surface staining of GluR1 and GluR2 in neurons after 30 minutes of DMSO or RA treatment. The staining was performed an hour after drug washout. Scale bar, 10 µm. (B) RA treatment increased surface GluR1 levels without affecting GluR2 levels (n = 10 neurons/group; *, $p < 0.0005$). (C) Biotinylation of surface GluR1 in primary cultured neurons after 30 minutes of DMSO or RA treatment, or after 24 hours of TTX+APV treatment. (D) Both RA treatment and activity blockade increased surface GluR1 expression, but no additional increase by RA following 24-hr TTX and APV treatment was observed (n = 3; *, $p < 0.01$). (E) and (F) RA-induced increase in synaptic transmission is completely blocked by Philanthotoxin-433 (PhTx, 5 µM) in dissociated hippocampal cultures (n = 8; *, $p < 0.05$). PhTx was bath-applied 10 minutes prior to the recording. Scale bar in E: 20 pA, 20 ms. (G) RA-induced increase in mEPSC amplitude in neurons from cultured slices was also sensitive to PhTx treatment (n = 10; *, $p < 0.01$). Single-factor ANOVA was used for all statistical analysis. Error bars represent SEM.

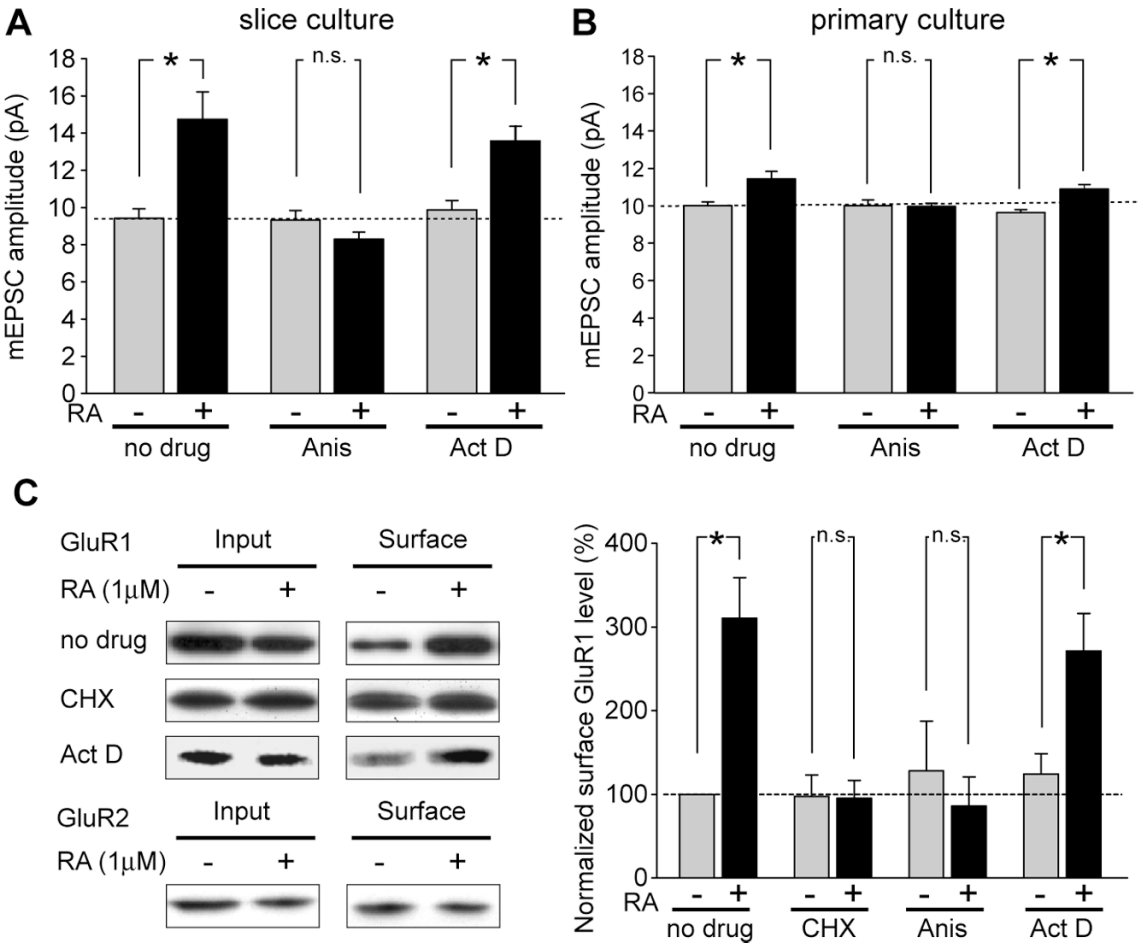

Figure 5. RA induced synaptic scaling is independent of transcription

(A) and (B) RA-induced synaptic scaling was blocked by the protein synthesis inhibitor anisomycin, but not by the transcription inhibitor actinomycin D in hippocampal pyramidal neurons from both slice culture (A) and dissociated culture (B) (n = 10/group; *, $p < 0.005$). Drug treatment was started 30 minutes prior to the RA treatment and was washed out together with RA. (C) Surface GluR1 levels in neurons were selectively increased by RA treatment, whereas GluR2 levels remained unchanged. The increase in GluR1 surface expression was blocked by either cycloheximide or anisomycin, but not by actinomycin D (n = 5; *, $p < 0.01$).

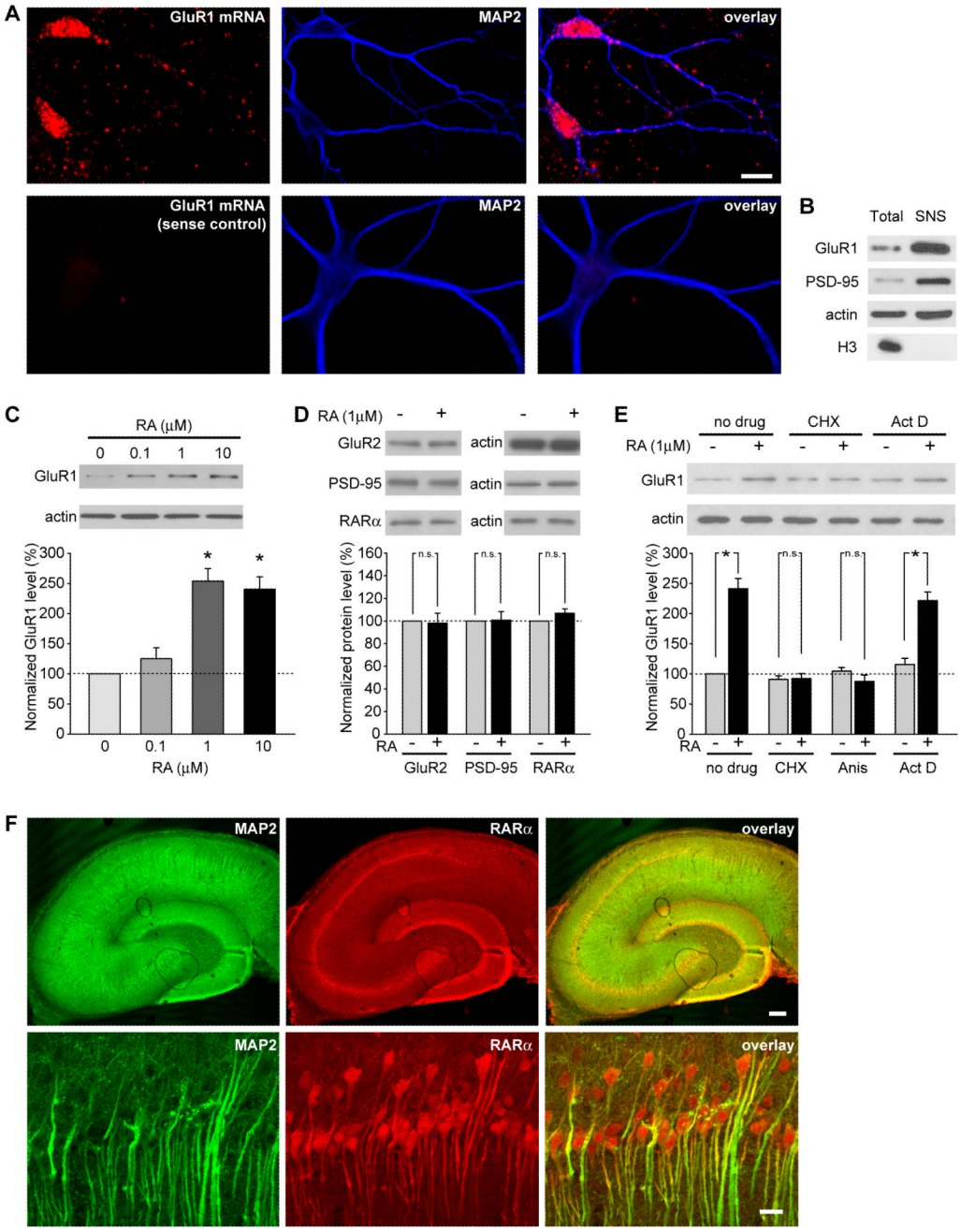

Figure 6. RA induces local translation of GluR1 proteins

(A) GluR1 mRNA was detected in neuronal dendrites as well as in glia cells. Antisense or sense probes against GluR1 mRNA (red) was used for fluorescent *in situ* hybridization. Neuronal soma and dendrites were labeled with MAP2 antibody (blue). Scale bar, 10 μm. (B) GluR1 and PSD-95 were enriched in, and histone H3 was selectively absent from, the hippocampal synaptoneurosome fraction relative to the whole-cell lysate. (C) Ten minute RA treatment (0.1, 1 or 10 μM) induced GluR1 synthesis in synaptoneurosomes (n = 4; *, $p < 0.005$). (D) GluR2, PSD-95 and RARα expression were not changed by RA treatment (n = 4, $p > 0.5$). (E) RA-induced GluR1 synthesis in synaptoneurosomes was blocked by cycloheximide and anisomycin, but not actinomycin D (n = 4; *, $p < 0.0005$). (F)

Immunofluorescence staining of hippocampal sections for MAP2 (green) and RARα (red; scale bar for upper panels, 200 μm; for lower panels, 20 μm).

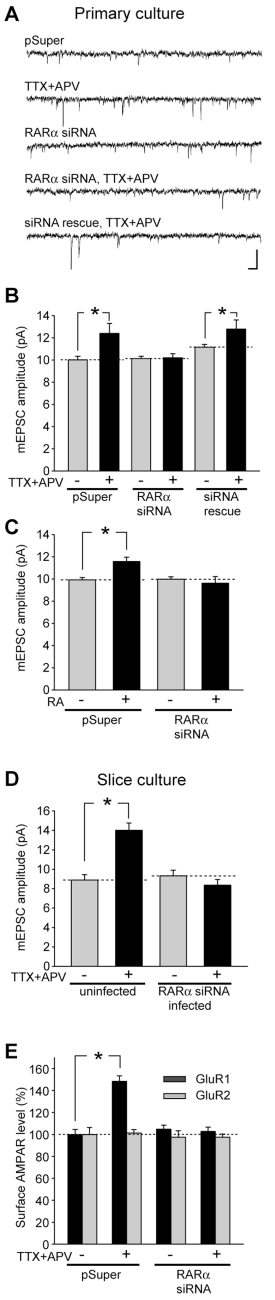

Figure 7. RARα is required for activity blockade- and RA-induced synaptic scaling

(A–C) Effect of RARα knockdown on activity blockade- and RA-induced synaptic scaling in primary cultured hippocampal neurons. (A) Representative traces of mEPSCs recorded from primary cultured neurons of various experimental groups. Scale bars: 20 pA, 20 ms. (B) Inactivity-induced synaptic scaling in dissociated cultures was blocked by RARα shRNA, and the impaired synaptic scaling was rescued by co-expression of a shRNA-resistant mutant RARα (n = 15/group; *, $p < 0.05$). (C) RA-induced synaptic scaling in dissociated cultures was blocked by RARα shRNA (n = 15/group; *, $p < 0.001$). (D) Activity blockade-induced synaptic scaling in cultured slices was blocked by RARα shRNA introduced with lentivirus (n = 10/group, $p < 1 \times 10^{-4}$). (E) Activity blockade induced a

significant increase in surface GluR1 but not GluR2 immunoreactivity, which was completely blocked by RARα knockdown (n = 50 dendrites from 18 neurons/group; *, $p < 1 \times 10^{-10}$).

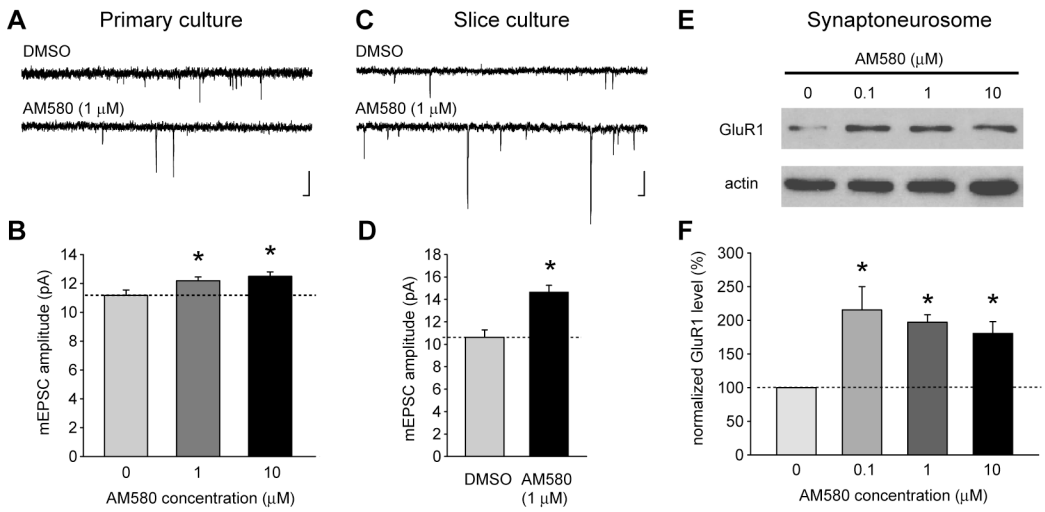

Figure 8. Pharmacological activation of RARα induces synaptic scaling and local GluR1 synthesis

(A–B) Treatment of dissociated hippocampal neurons in culture with the RARα-specific agonist AM580 (1 μM) induced synaptic scaling in neurons from dissociated cultures in a dose-dependent manner (n = 10/group; *, $p < 0.05$). Scale bars: 20 pA, 20 ms. (C–D) Treatment of cultured hippocampal slices with 1 μM AM580 significantly increased mEPSC amplitude of neurons (n = 16/group, $p < 1 \times 10^{-4}$). Scale bars: 20 pA, 20 ms. (E–F) AM580 increased GluR1 synthesis in hippocampal synaptoneurosomes (n = 5; *, $p < 0.005$).

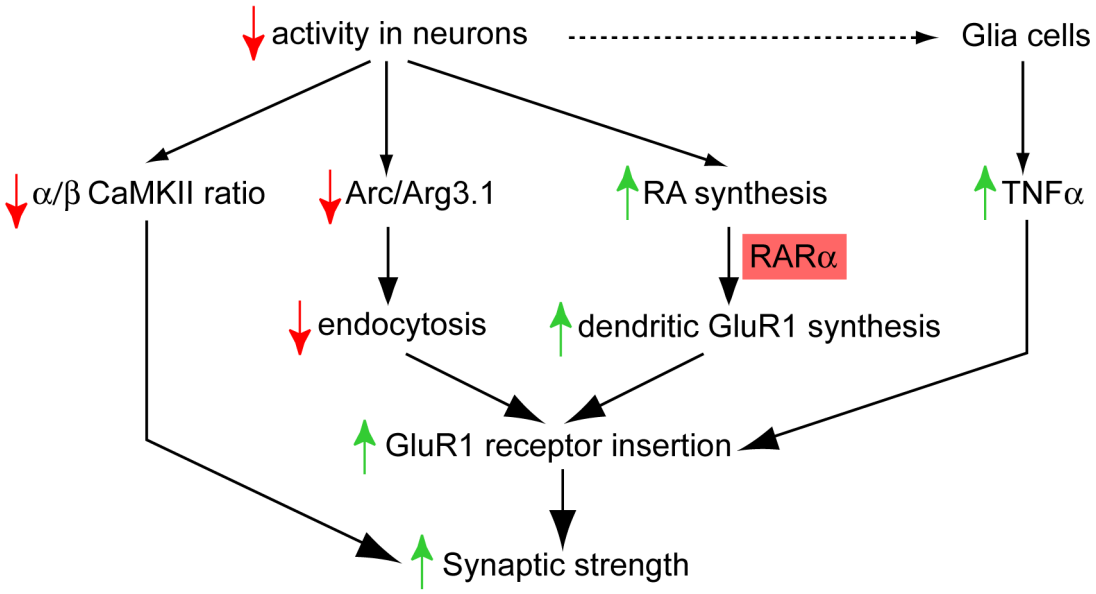

Figure 9. Signaling pathways in homeostatic synaptic plasticity induced by neuronal activity blockade

Previous studies showed that a reduction in neuronal activity (top), which ultimately produces an increase in synaptic strength (bottom), causes changes in intracellular proteins Arc/Arg3.1 and CaM Kinase II (middle; (Shepherd et al., 2006; Thiagarajan et al., 2002), and induces TNFα secretion from glia cells (right; (Stellwagen and Malenka, 2006). We here propose that in addition to these pathways that were previously shown to be required for the particular forms of plasticity studied, activity blockade also induces an increase in RA synthesis, which signals through RARα, directly or indirectly stimulates the insertion of more GluR1-type AMPA-receptors. As a result, even with reduced neuronal activity, the increased strength of individual synapses as a consequence of activation of these pathways leads to the same overall level of synaptic transmission.